European Journal of Medicinal Chemistry 53 (2012) 64–75

Contents lists available at SciVerse ScienceDirect

European Journal of Medicinal Chemistry

journal homepage: http://www.elsevier.com/locate/ejmech

Original article

Isoxazolo(aza)naphthoquinones: A new class of cytotoxic Hsp90 inhibitors

Alberto Bargiotti [a], Loana Musso [a], Sabrina Dallavalle [a,*], Lucio Merlini [a], Grazia Gallo [b], Andrea Ciacci [b], Giuseppe Giannini [b], Walter Cabri [b], Sergio Penco [b], Loredana Vesci [b], Massimo Castorina [b], Ferdinando Maria Milazzo [b], Maria Luisa Cervoni [b], Marcella Barbarino [b], Claudio Pisano [b], Chiara Giommarelli [c], Valentina Zuco [c], Michelandrea De Cesare [c], Franco Zunino [c]

[a] Dipartimento di Scienze Molecolari Agroalimentari, Università di Milano, Via Celoria 2, 20133 Milano, Italy
[b] Sigma-tau, R&D, Via Pontina km 30400, 00040 Pomezia, Italy
[c] Unità di Chemioterapia e Farmacologia Antitumorale Preclinica, Dipartimento di Oncologia Sperimentale e Laboratori, Fondazione IRCCS Istituto Nazionale dei Tumori, Via Venezian 1, 20133 Milano, Italy

ARTICLE INFO

Article history:
Received 2 December 2011
Received in revised form
28 January 2012
Accepted 20 March 2012
Available online 28 March 2012

Dedicated to the memory of Dr. Paolo Carminati.

Keywords:
Synthesis
Isoxazolonaphthoquinones
Hsp90 inhibitors
Antitumour
Antiproliferative activity
QSAR

ABSTRACT

A series of 3-aryl-naphtho[2,3–*d*]isoxazole-4,9-diones and some of their 6-aza analogues were synthesized and found to inhibit the heat shock protein 90 (Hsp90). The compounds were tested for their binding to Hsp90 and for their effects on Hsp90 client proteins expression in a series of human tumour cell lines. Representative compounds (**7f**, **10c**) downregulated the Hsp90 client proteins EGFR, Akt, Cdk4, Raf-1, and survivin, and upregulated Hsp70. Most of the compounds, in particular the alkylated 3-pyridyl derivatives, exhibited potent antiproliferative activity, down to two-digit nanomolar range. Preliminary results indicated *in vivo* activity of **7f** against human epithelial carcinoma A431 model growing as tumour xenograft in nude mice, thus supporting the therapeutic potential of this novel series of Hsp90 inhibitors.

1. Introduction

The interest for the heat shock protein 90 (Hsp90) as a therapeutic target is related to its central role in correct folding and stabilization of proteins involved in malignant behaviour and tumour progression [1]. Multiple signal transduction pathways implicated in the regulation of cell proliferation and survival are dependent on Hsp90 [2]. Several Hsp90 client proteins are involved in critical processes including cell-cycle regulation and apoptosis [3]. The heat shock proteins are often overexpressed in tumour cells, and this supports their ability to survive under unfavourable stress conditions (e.g. hypoxia and acidosis). The essential chaperoning function of Hsp90 is subverted during oncogenesis to make malignant transformation possible and to facilitate rapid somatic evolution [3]. Functioning as a biochemical buffer for the numerous genetic lesions that are present within tumours, Hsp90 allows mutant proteins to retain or even gain function, while permitting cancer cells to tolerate the imbalanced signalling that such oncoproteins create. Thus, targeting Hsp90 may have the potential advantage of simultaneously blocking multiple oncogenic pathways [4].

Hsp90 exists as a homodimer made up of three domains [1,2]. The N-terminal domain contains an ATP-binding site that binds the natural products geldanamycin and radicicol, and the analogue 17-AAG (Chart 1). The middle domain is highly charged and has high affinity for cochaperones and client proteins. A second ATP-binding site is located in the C-terminus of Hsp90. This C-terminal nucleotide binding pocket has been shown to bind not only ATP, but cisplatin, novobiocin, epigallocatechin-3-gallate (EGCG) and taxol [5].

A number of highly specific Hsp90 inhibitors have been identified [6]. They redirect Hsp90 chaperoning activity and decrease cellular levels of its numerous cancer-related client proteins [2]. Such inhibitors exhibit promising antitumour activity as single

* Corresponding author. Tel.: +39 (2) 50316818; fax: +39 (2) 50316801.
E-mail address: sabrina.dallavalle@unimi.it (S. Dallavalle).

0223-5234/$ – see front matter © 2012 Elsevier Masson SAS. All rights reserved.
doi:10.1016/j.ejmech.2012.03.036

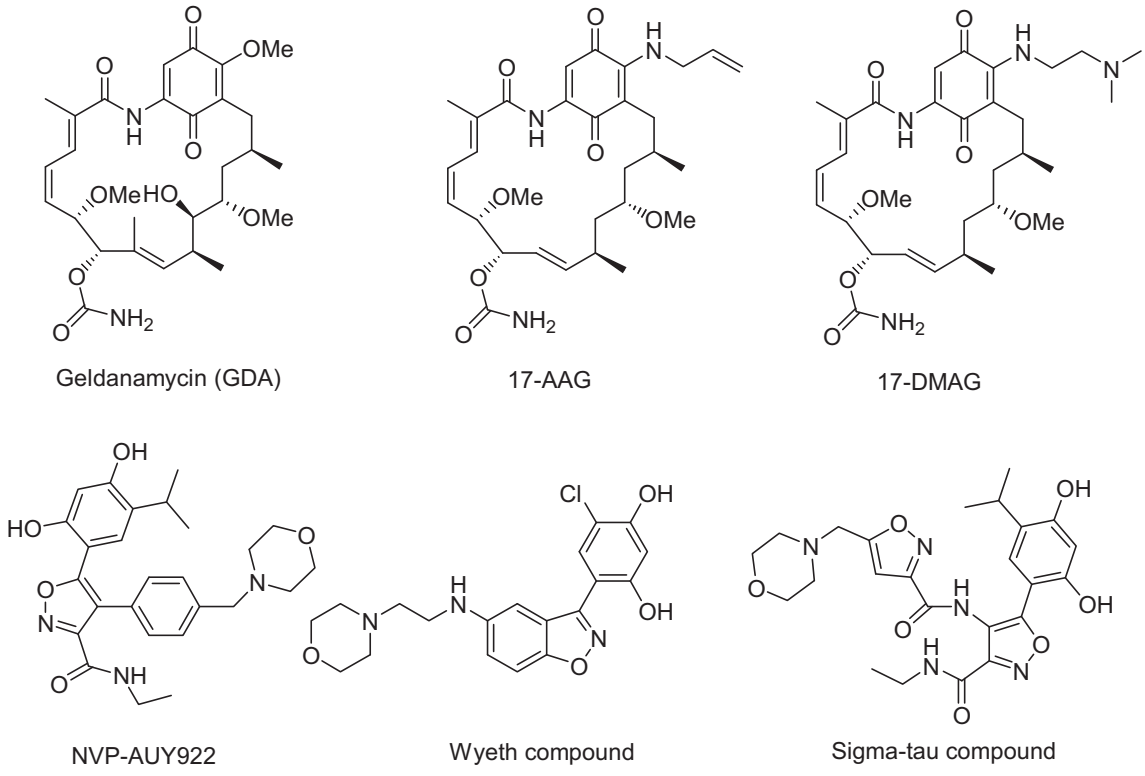

Chart 1.

agents or in combination with other cytotoxic agents [7–9], and some of them are in clinical development [10,11]. Geldanamycin, the first Hsp90 inhibitor discovered, and its derivatives 17-AAG (tanespimycin) and 17-DMAG (17-dimethylamino-ethylamino-17-demethoxygeldanamycin, alvespimycin), that have entered clinical trials, are ansa compounds containing a key aminoquinone moiety [12]. (Chart 1).

Quinones are a class of organic compounds endowed with a variety of biological activities, mostly connected with their redox properties. A number of natural and synthetic quinones show remarkable anticancer activity [12], and a series of synthetic 1,4-naphtoquinones have recently been identified as Hsp90 inhibitors [13].

Moreover, among the large number of Hsp90 inhibitors, some compounds, containing the isoxazole nucleus (Chart 1), have shown potent and selective inhibition of this molecular chaperone [14]. The presence of the heterocyclic nucleus seems to exert a role in the docking of the compounds to the ATP-binding site of Hsp90 [15].

This paper reports the synthesis and the assessment of the cytotoxic activity of a series of new isoxazolo-fused naphthoquinones and isoquinolinoquinones, that exert their antitumour activity via inhibition of the molecular chaperone Hsp90.

2. Chemistry

The 1,3-dipolar cycloaddition of benzonitriloxides to quinones is a well–known reaction [16] that has been exploited for the synthesis of simple and substituted isoxazolo-fused quinones [17] and naphthoquinones [18]. Thus, the first series of compounds (**3a**–**p**) was prepared reacting the naphthoquinone **1** with the nitrile oxides obtained in situ by treating the corresponding oximes **2** with triethylamine and aqueous NaClO in dichloromethane [19] (Schemes 1 and 2).

Some compounds (**3c**,**f**,**h**,**i**) were prepared by demethylation of the corresponding ethers (**3b**,**e**,**g**). Compounds **6a**–**e** were obtained regioselectively [20] by 1,3-dipolar cycloaddition on the

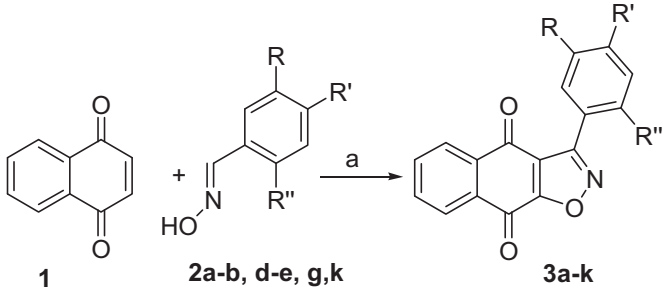

Scheme 1. Reagents and conditions: a) TEA, 15% NaClO, CH_2Cl_2, 0 °C, 1.5 h; b) HBr 35%, AcOH, reflux, 5 h; c) BBr_3, CH_2Cl_2, 0 °C, 1 h, then rt, 30 min; d) BBr_3, CH_2Cl_2, 0 °C, 1.5 h, then rt, 1 h; e) HBr 35%, AcOH, reflux, 48 h.

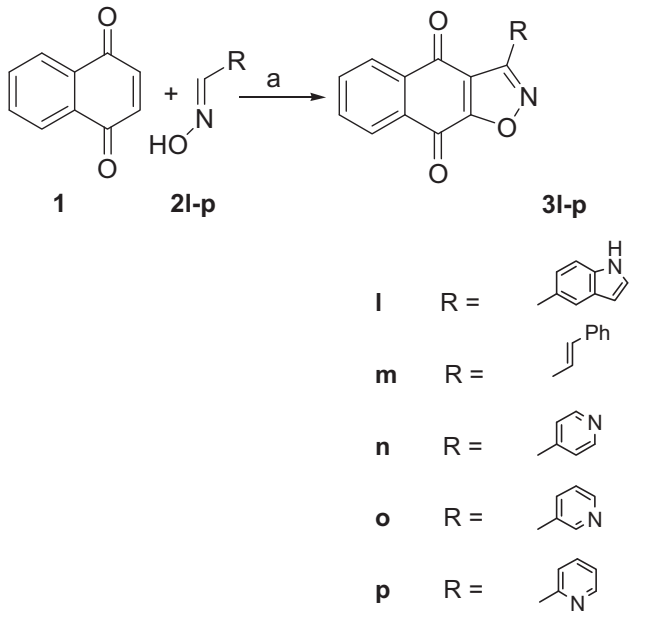

Scheme 2. Reagents and conditions: a) TEA, 15% NaClO, CH_2Cl_2, 0 °C, 1.5 h.

bromonaphthoquinones **5** [21], followed in the case of **6b** and **6e** by the hydrolysis of the corresponding acetate (**6a**, **6d**) (Scheme 3).

The pyridino derivatives **3n**–**p** and **6c**–**e** were alkylated with benzyl bromide or 2-bromomethylpyrazine in DMSO, or by iodomethane in methanol, to obtain the quaternary salts **7a**–**i** (Scheme 4).

Reduction of the naphthoquinones to the corresponding hydroquinones gave unstable compounds, so that two of them (**3b**, **d**) were transformed into the hydroquinone diacetates (**8a**–**b**) by reaction with Zn and acetic acid (Scheme 5).

As the isoquinolinone nucleus is present in some natural (e.g. calothryxin [22] and cribrostatin 6 [23]) and synthetic [24] cytotoxic compounds, we planned to introduce this moiety in place of the naphthoquinone nucleus. For this purpose 6-bromo-2-azanaphthoquinone **9** was prepared by bromination of 5-

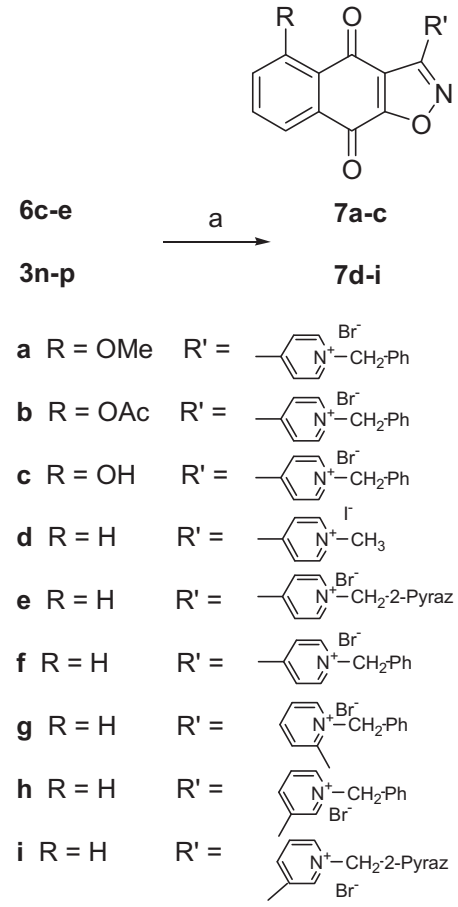

Scheme 4. Reagents and conditions: a) For **7a**–**c**,**f**–**h**: benzyl bromide, DMSO, rt, overnight; for **7d**: MeI, MeOH, rt, overnight; for **7e**,**i** : 2-bromomethylpyrazine, DMSO, rt, 72 h.

hydroxyquinoline [25], followed by oxidation of the resulting dibromoderivative [26]. The 1,3 dipolar cycloaddition was carried out following the conditions previously described for the synthesis of the isoxazolonaphthoquinones (Scheme 6). The reaction

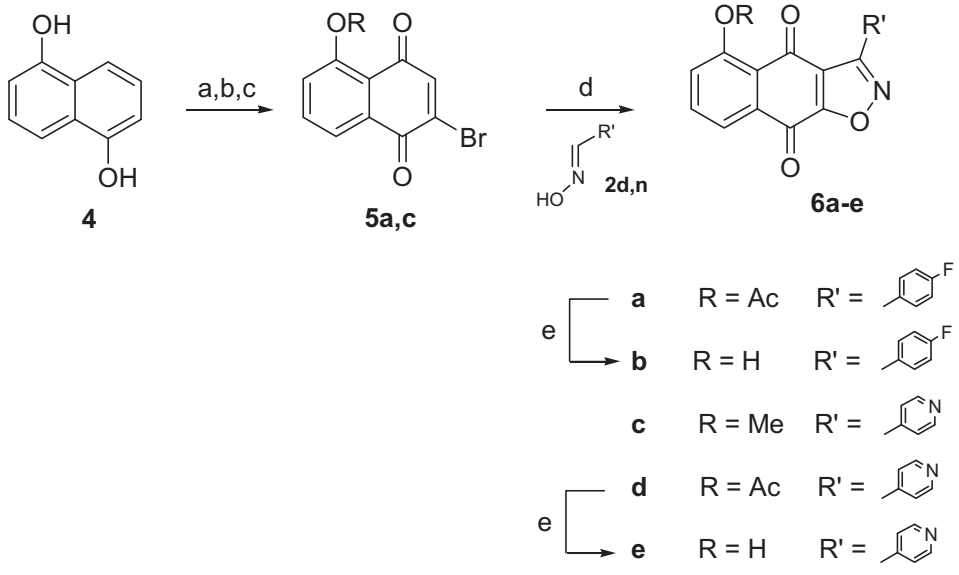

Scheme 3. Reagents and conditions: a) Ac_2O, Py, rt, 3 h; b) NBS, AcOH/H_2O, 50 °C, 2 h; c) for **5c**: i) H_2SO_4 1.5 M, EtOH, reflux, 3 h; ii) MeI, Ag_2O, CH_2Cl_2, rt, overnight; d) TEA, 15% NaClO, CH_2Cl_2, 0 °C, 1.5 h; e) K_2CO_3, H_2O/MeOH, rt, 40 min.

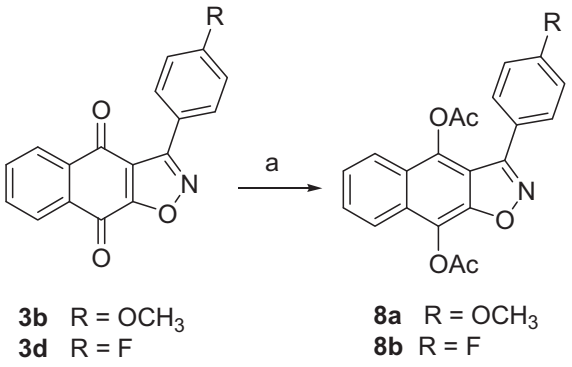

Scheme 5. Reagents and conditions: a) Zn powder, TEA, acetic anhydride, reflux, 3 h.

appeared regioselective, giving only the isomers with structure **10a**–**d**, as confirmed by NMR spectra.

3. Results and discussion

The prepared compounds were tested in a binding assay for their affinity to Hsp90 and for their antiproliferative activity on a number of human tumour cell lines (non small-cell lung cancer NCI-H460, squamous-cell carcinoma A431, peritoneal mesothelioma STO) (Table 1).

In general, some of the compounds tested showed strong antiproliferative activity, comparable to or even higher than the activity of 17-AAG, especially on the carcinoma cells A431. Among the naphthoisoxazolediones, a number of them showed strong binding to Hsp90 (**3n**,**o**, **6b**,**d**, **7a**–**f**,**h**,**i**), with some correlation with the antiproliferative activity. The presence of a substituent in the *ortho* position on the phenyl ring had a deleterious effect (**3f**–**i**), possibly due to steric hindrance. The pyridine derivatives (**3n**–**p**, **6c**–**d**) showed a better binding and stronger activity than the corresponding phenyl derivatives (**3a**,**b**,**6a**,**b**), although the introduction of an OH group on the naphthoquinone ring has opposite effects in the two series (**6e** vs. **6b**).

The two hydroquinone acetates **8a**,**b** showed a very weak binding affinity, and low antiproliferative activity.

Change of the naphthoquinone to an isoquinolinone nucleus led to an improvement both of binding affinity and of antiproliferative activity (**10a**–**d**) with respect to the corresponding naphthoquinone derivatives (see for ex. **10c** vs **3k**). Compound **10c**, that contains a polar, hydrophilic morpholino group, was the most active compound of the series in terms of Hsp90 binding. Relevant to this point is the observation that the morpholine moiety is present in all the most active isoxazole-containing compounds reported in the literature [14] (see chart 1).

Table 1
Binding affinity to Hsp90 and antiproliferative activity for the prepared compounds.

Cpd.	Binding Hsp90 (FP) IC_{50}±SD [μM]	NCI-H460 IC_{50}±SD [μM] 72 h	STO IC_{50}±SD [μM] 72 h	A 431 IC_{50}±SD [μM] 72 h
17-AAG	1.095 ± 0.05	0.010 ± 0.002	–	0.069 ± 0.005
3a	7.85 ± 0.04	0.12 ± 0.03	0.02 ± 0.004	0.12 ± 0.008
3b	5.84 ± 0.04	0.65 ± 0.03	0.16 ± 0.04	0.35 ± 0.03
3c	>100	0.51 ± 0.004	0.46 ± 0.17	0.21 ± 0.01
3d	>100	0.35 ± 0.02	0.02 ± 0.02	0.26 ± 0.011
3e	>100	0.29 ± 0.001	0.66 ± 0.04	0.13 ± 0.01
3f	1.55 ± 0.024	>1	3.4 ± 0.1	3.4 ± 0.7
3g	>100	0.88 ± 0.07	0.135 ± 0.06	1.4 ± 0.3
3h	>100	>1	0.30 ± 0.08	2.98 ± 0.40
3i	4.2 ± 0.01	>1	1.0 ± 0.1	23.0 ± 7.2
3k	1.2 ± 0.1	0.866 ± 0.031	1.13 ± 0.1	0.44 ± 0.21
3l	>100	0.30 ± 0.01	0.32 ± 0.04	0.32 ± 0.08
3m	>100	>1 (40%)	0.12 ± 0.1	0.32 ± 0.12
3n	0.39 ± 0.01	0.14 ± 0.02	0.011 ± 0.04	0.056 ± 0.005
3o	0.54 ± 0.009	0.062 ± 0.003	0.04 ± 0.02	0.043 ± 0.001
3p	1.06 ± 0.01	1.0 ± 0.05	0.02 ± 0.01	0.34 ± 0.09
6a	1.94 ± 0.01	0.078 ± 0.005	1.05 ± 0.68	0.27 ± 0.01
6b	0.29 ± 0.01	0.124 ± 0.009	0.61 ± 0.05	0.29 ± 0.22
6c	1.9 ± 0.1	0.88 ± 0.07	0.261 ± 0.060	0.33 ± 0.03
6d	0.084 ± 0.001	0.15 ± 0.04	0.150 ± 0.080	0.06 ± 0.01
6e	>100	0.88 ± 0.07	0.103 ± 0.120	0.068 ± 0.010
7a	0.34 ± 0.01	0.18 ± 0.01	0.168 ± 0.090	0.168 ± 0.01
7b	0.031 ± 0.001	>1 (32%)	3.96 ± 0.20	3.96 ± 0.6
7c	0.098 ± 0.001	0.88 ± 0.07	21.56 ± 0.90	21.6 ± 0.7
7d	0.63 ± 0.01	0.33 ± 0.01	1.20 ± 0.05	0.48 ± 0.06
7e	0.68 ± 0.01	0.017 ± 0.001	0.22 ± 0.05	0.052 ± 0.001
7f	0.034 ± 0.002	0.018 ± 0.0007	0.0022 ± 0.0010	0.0016 ± 0.0010
7g	>100	>1	2.24 ± 0.80	2.24 ± 0.07
7h	0.77 ± 0.009	0.021 ± 0.001	0.01 ± 0.06	0.020 ± 0.0009
7i	0.51 ± 0.01	0.046 ± 0.004	0.11 ± 0.05	0.042 ± 0.002
8a	>100	>1 (39%)	1.00 ± 0.04	1.30 ± 0.03
8b	>100	>1	0.67 ± 0.21	0.69 ± 0.22
10a	5.6 ± 0.1	0.183 ± 0.01	0.004 ± 0.001	0.004 ± 0.002
10b	1.6 ± 0.1	0.446 ± 0.042	0.092 ± 0.022	0.098 ± 0.036
10c	<0.005[a]	0.041 ± 0.004	0.054 ± 0.01	0.02 ± 0.01
10d	0.12 ± 0.01	0.085 ± 0.0009	0.06 ± 0.018	0.0085 ± 0.0033

[a] For the detection limits of the assay, see Chiosis et al. [27].

To increase the polarity and possibly the water solubility, the pyridine derivatives **3n**–**p** and **6c**–**e** were alkylated with benzyl or methyl or 2-pyrazinylmethyl halides, to give the corresponding quaternary salts **7a**–**i**. This modification led to a general increase in the binding affinity, especially for **7b**,**c**,**f**, all exhibiting submicromolar values. With the exception of **7b**,**7c** and of **7g** (where again the alkylation on the ortho position was detrimental), these compounds were characterized by a potent antiproliferative activity with nanomolar IC_{50} values.

The most potent compounds of the whole series, **7f** and **10c**, were tested for their ability to downregulate the expression of Hsp90 client proteins in the squamous cell carcinoma A431 and the mesothelioma STO cells (Fig. 1). After 24–h exposure to

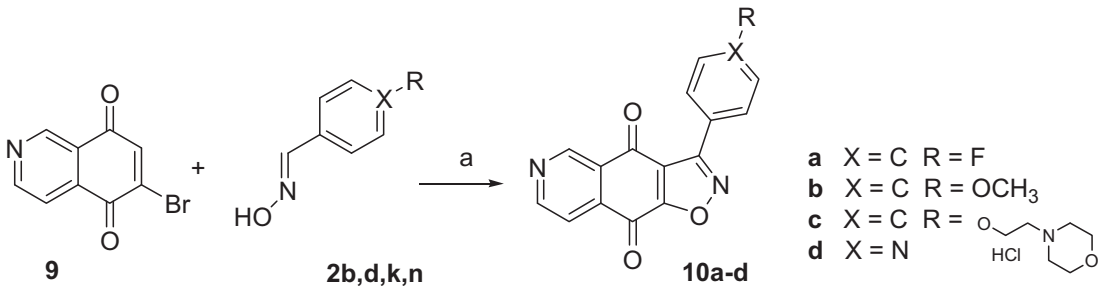

Scheme 6. Reagents and conditions: a) TEA, 15% NaClO, CH_2Cl_2, 0 °C, 1.5 h.

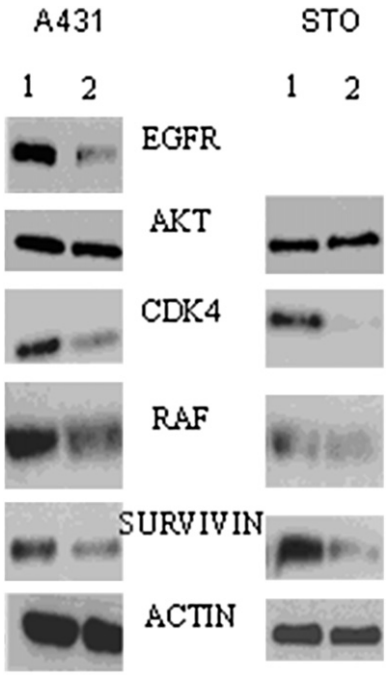

Fig. 1. Analysis of Hsp90 client protein levels in A431 and STO cells after 24 h of treatment with **7f**. EGFR, survivin, Cdk4, Akt and Raf-1 levels. Total cellular extracts were obtained 24 h after cell treatment (**7f**, 22 nM, IC_{80}). Actin is shown as a control for protein loading. Lane 1: control; lane 2: **7f**.

a cytotoxic concentration of **7f**, Western blot analysis indicated depletion of Cdk4, Raf and survivin in both cell lines. Moreover, the treatment with **7f** caused an almost complete depletion of EGFR protein in A431 cells, which exhibited overexpression of the receptor.

Analogously, **10c** caused a dramatic and dose-dependent depletion of Akt, CDK-4, survivin and EGFR in A431 cells (Fig. 2). Thus, the modulation of Hsp90 client proteins was consistent with inhibition of Hsp90 function. Moreover, Fig. 3 reports Hsp70 protein expression modulation in A431 cells following exposure to **7f** or of **10c**. This dose-dependent upregulation of Hsp70 cochaperone is consistent with the target Hsp90 modulation [28].

The observation that compounds which exhibited high binding affinity (e.g. **7f**, **6d**, **10c**) are also potent as cytotoxic agents supports that Hsp90 is a cellular target implicated in the antiproliferative/antitumour effects of some compounds of this series. The

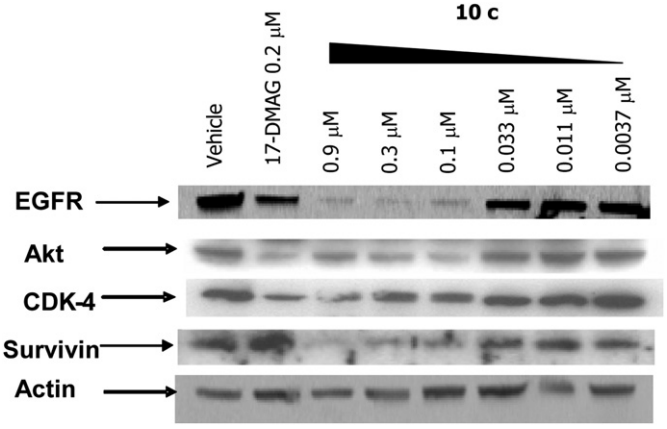

Fig. 2. Analysis of Hsp90 client protein levels in A431 cells after treatment with different concentrations of **10c**. Actin is shown as a control for protein loading.

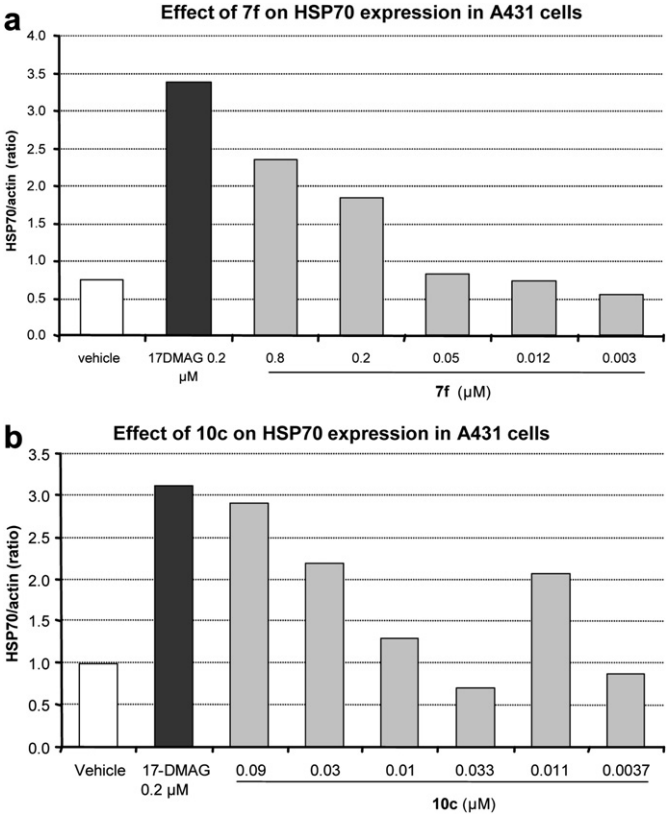

Fig. 3. Analysis of Hsp70 expression in A431 tumour cells treated with compounds **7f** (a) and **10c** (b). Western blot analysis was performed on total cellular extracts after 24 h of treatment. Results of densitometry analysis were reported as normalized (to β-actin) ratios.

biochemical analysis of Hsp90 client expression modulation is consistent with this interpretation.

However, some compounds, although strongly binding the enzyme, show low antiproliferative activity. In this case the chemico-physical features of the compounds may influence the cellular pharmacokinetic behaviour and therefore cellular response (compare **7b** with **7f**).

On the contrary, the appreciable cell growth inhibition by compounds (e.g. **3c**–**e**, **6e**) which did not exhibit a strong Hsp90 interaction suggests that other off-target effects are likely involved in the mechanism of action of compounds of this class.

By virtue of their quinone moiety, the benzoquinone ansamycin class of Hsp90 inhibitors can undergo bioreduction to hydroquinone forms by action of NAD(P)H:quinone oxidoreductase 1 (NQO1), a FAD-dependent direct two-electron reductase that can use either NADH or NADPH as reducing cofactor and reduces quinones directly to hydroquinones [29]. Relatively high levels of NQO1 protein have been detected in many human solid tumours, including lung, breast, colon, ovary, and pancreas [30]. Hydroquinone forms of 17AAG and 17DMAG are relatively stable, but they have been shown to be sensitive to copper-mediated reoxidation [31]. Hydroquinone forms of 17-AAG and 17-DMAG have also been shown to be more potent inhibitors of Hsp90 in *in vitro* studies using purified Hsp90 compared with their parent quinones [32,33]. It appears thus established that NQO1 acts as an important factor to modulate the Hsp90 inhibitory activity of anticancer quinones [1,33]. Other data also illustrate the close relationship between Hsp90 regulation and cellular redox homeostasis, pointing to the role of oxidative stress, such as induced by quinones, in the disruption of the Hsp90 signalling complex [34]. Therefore it

cannot be excluded that also our compounds may modulate Hsp90 function via NQO1.

On the basis of the cellular/biochemical profile of activity, the therapeutic effect of **7f** was determined in the A431 model growing as tumour xenograft in nude mice. Using oral administration, daily treatment for 3 weeks with **7f** produced an appreciable inhibition of tumour growth, i.e. 50–65% in two independent experiments (Fig. 4).

4. Molecular modelling and QSAR study

Docking studies were performed using three different conformations/crystal structures of Hsp90 (PDB code: 1UY6 for helical conformation; 2BYH for open conformation and 2VCI for closed conformation). The best solutions were found using Hsp90 helical conformation.

Thus, we compared the orientation of our most active compounds in the Hsp90 active site with the orientation of SNX2112 [35], a compound in clinical development, co-crystallized in the helical conformation. Fig. 5 shows the superimposition of **7f** and SNX2112 where the common interactions are represented by quinone group vs. carbonyl function of the amide group and by the heteroaromatic substituents of the two structures filling the internal pocket behind the helix.

Additional interaction for **7f** is found between the isoxazole group and a conserved water molecule, while the interaction with Asp93 is not retrieved due to the absence of H-bond donor groups.

Comparison with 17-DMAG and NVP-AUY922 is shown in the SI.

An attempt to correlate the structural relationships of the compounds described above with the binding to Hsp90 was made using pharmacophore modelling and 3D quantitative structure–activity relationships (3D-QSAR). Then, in this study, the generation of a pharmacophore for the Hsp90 binding allowed us to determine the molecular components required for activity and 3D-QSAR allowed us to predict Hsp90 activity values.

Table 2 shows the compounds (27) tested for the generation of the three-dimensional (3D) pharmacophore model in order to rationalize chemical structure with the observed binding affinities of the 4,9-dioxo-4,9-dihydronaphtho[2,3–b]isoxazoles. Compounds with $pIC_{50\ FP} > 7.3$ (an arbitrarily chosen activity threshold of 50 nM) were assigned to the active class (3 compounds) and used in the development of the pharmacophore.

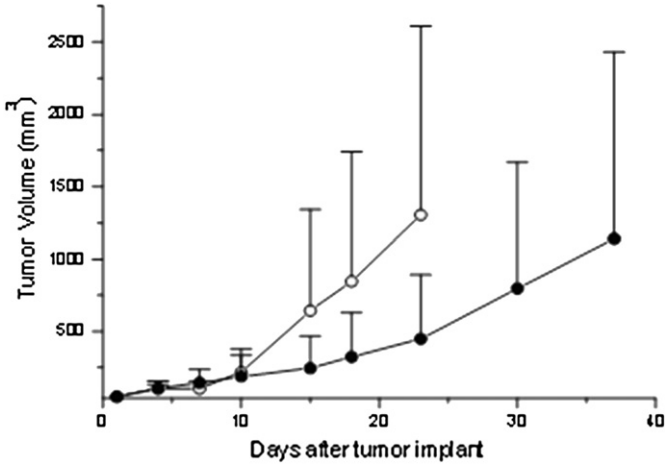

Fig. 4. Antitumor activity of **7f** against the squamous cell carcinoma A431 xenograft in nude mice. The compound, **7f**, dissolved in physiologic saline was administered p.o. (10 mg/kg) for four consecutive days/week (●). The treatment started when the tumours were just palpable, was repeated for three weeks (i.e., qdx4d/week x 3 weeks). (○), untreated controls.

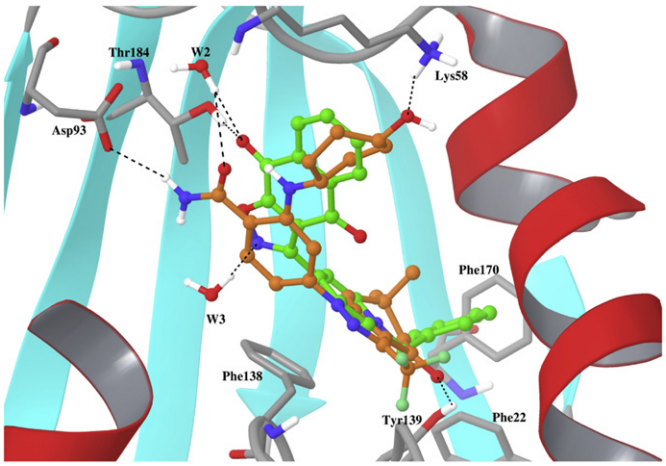

Fig. 5. Docking pose of compound **7f** (green) and **SNX2112** (orange) in Hsp90 active site (helical conformation). H-bonds are shown as dotted lines. (For interpretation of the references to colour in this figure legend, the reader is referred to the web version of this article.)

A comprehensive conformational search was generated for each of the 27 molecules, sampling the conformational space that may represent possible active structures. Conformers beyond 8.3 kJ/mol (2 kcal/mol) of the global minimum were automatically discarded. Visual inspection and careful analysis of chemical features were conducted to guide the pharmacophore development process.

Particular attention was paid to compound **10c**, as it represents the most active derivative. Five-membered and six-membered heterocyclic rings were replaced with a single, custom group feature (X) representing this functional group. Pharmacophore variants considered for Hsp90 inhibition were composed of four chemical features: hydrogen-bond acceptor (A, pink sphere), aromatic ring (R, ring), hydrophobic (H, green sphere), and heterocyclic ring (X, blue sphere in order to avoid that aromatic

Table 2
Binding to Hsp90 (Hsp90 (FP) IC_{50}, μM), pIC_{50} (FP), predicted pIC_{50} (FP) and set of selected compounds used for QSAR analysis.

Cpd.	Binding Hsp90 (FP) IC_{50}[μM]	pIC_{50} (FP)	Pred. pIC_{50}	QSAR set
3a	7.85	5.11	4.87	training
3d	200	3.7	4.87	training
3f	1.55	5.81	5.29	training
3i	4.2	5.38	5.09	training
3k	1.2	5.92	5.85	training
3n	0.39	6.41	6.30	training
3p	1.06	5.97	5.73	training
6b	0.29	6.54	6.02	training
6c	1.9	5.72	6.47	training
6d	0.084	7.08	7.11	training
7d	0.63	6.2	6.23	training
7f	0.034	7.47	7.38	training
7g	200	3.7	3.8	training
7i	0.51	6.29	6.25	training
10a	5.6	5.25	5.7	training
10b	2.45	5.61	5.78	training
10c	<0.005	8.47	8.69	training
10d	0.12	6.92	6.36	training
3b	5.84	5.23	5.49	test
3e	200	3.7	5.13	test
3l	1.94	5.71	5.76	test
3o	0.54	6.27	5.3	test
7a	0.34	6.47	7.28	test
7b	0.031	7.51	7.51	test
7c	0.098	7.01	6.64	test
7e	0.68	6.17	6.98	test
7h	0.77	6.11	6.56	test

rings were misplaced) with at least six sites. Common pharmacophores exhibiting AAHRRX were searched in all actives with a final box size and minimum intersite distance of 1.0 Å. Two hypotheses were generated, and that with the best score (Survival = 3.163 based on the PHASE scoring functions [36,37]) was chosen as the final Hsp90 pharmacophore for use in subsequent 3D-QSAR investigation. The identified variant assigned a single site, X, to the isoxazole ring; the hydrogen bond acceptor sites (A), corresponded to the 4,9-dioxo groups; aromatic features (R) was placed on the naphthoquinone aromatic ring and on the first ring of the isoxazole substituent; finally, a hydrophobic feature (H) corresponded to aromatic or alkyl group at the end of substituent. While not essential for activity, molecules lacking hydrophobic features generally show a decrease in pIC_{50}. Apart from correctly identifying the active compounds, the pharmacophore was used to prealign the molecules for QSAR analysis.

Attempts to statistically analyse three-dimensional molecular fields by means of a QSAR analysis were made: molecules reported in Table 2 were placed into training and test sets once aligned onto the pharmacophore (see Fig. 6) with an effort to minimize structural redundancy while maximizing coverage of the experimental activities. The training and test sets were composed of 18 and 9 molecules respectively. Atom based QSAR model was built using a grid spacing of 1.0 Å, two partial least-squares (PLS) factor and eliminating variables with |t-value| < 2.0.

The performance of the two PLS factors atom-based QSAR model on the training and test set molecules is illustrated in Fig. 7. The scatter plot indicates good correlation coefficients (Stability = 0.64; R^2 = 0.81 and Q^2 = 0.64), indicative of a model with strong predictive power and significance.

Table 2 also compares experimental and predicted pIC_{50} values for both the training and test set molecules, showing that activity was effectively predicted. This observation further supports the validity of the pharmacophore model, suggesting that the spatial arrangement of chemical features, when aligned by the pharmacophore, is indicative of the probable active conformation of the molecule. Although good predictive power is evident, the low number of training/test set compounds warrants caution when using this model for this purpose.

Fig. 8 provides a visual representation of the atom-based 3D-QSAR model (global, hydrophobic/non polar, positive ionic, and electronegative) represented by colour codes.

The global regions of favourable and unfavourable interactions are represented in Fig. 8a. Hydrophobic contributions are shown in Fig. 8b; the map showed a big green coloured region indicating that an increase in the hydrophobicity in this region is expected to improve the activity of the dioxodihydronaphtho[2,3−b]isoxazole

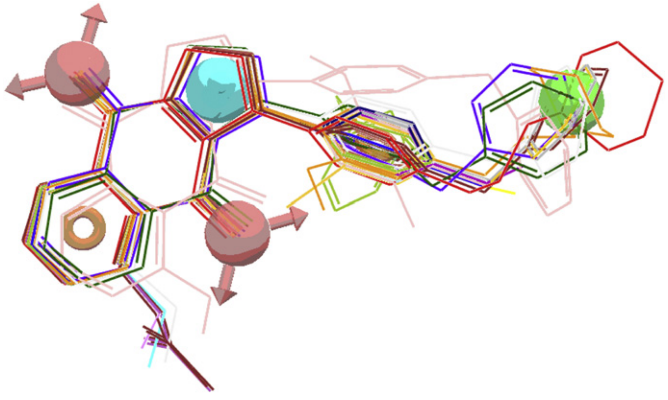

Fig. 6. Pharmacophore for Hsp90 inhibition with overlay of the whole set of compounds.

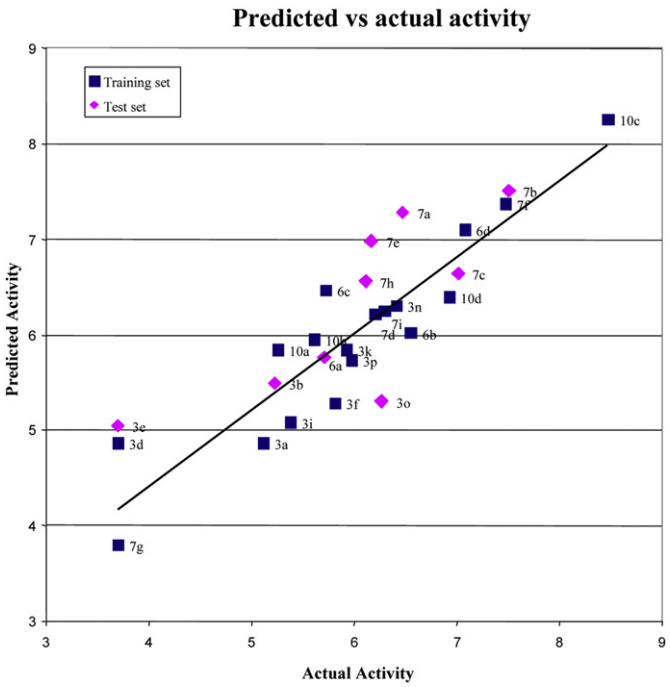

Fig. 7. Scatter plot of predicted vs actual Hsp90 binding activity applied to 27 compounds.

derivatives (see for example compound **3n** vs **7f**). A purple coloured region corresponding to the *ortho*-substituent of 3-phenyl ring disfavours the placement of hydrophobic groups (see for example compound **7g** vs **7f**,**7h**). Positive ionic contributions are shown in Fig. 7c; the map showed that the 4-pyridinium group is favoured vs. 2-pyridinium one (see for example compound **7g** vs **7f**). Electronegative contributions are shown in Fig. 7d. The map describes the spatial arrangement of favourable electron-withdrawing atoms: the atom 6 (see compound **3n** vs **10d**) and C5 position (see compound **3n** vs. **6d**) of dihydronaphtho[2,3−b] isoxazole, the *para* position of the aromatic ring in C3 (see compound **3a** vs **3n**) and the region occupied by morpholine oxygen atom in the most active molecule (see compound **7f** vs **10c**).

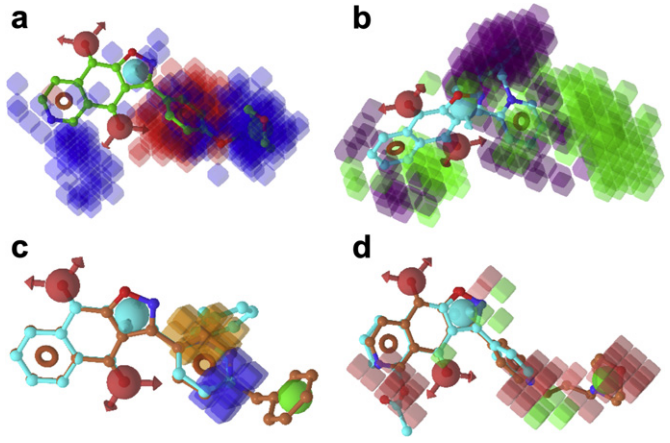

Fig. 8. Visual representation of atom-based PHASE QSAR model: a) Global model (colour code: blue, positive; red, negative); b) Hydrophobic/non-polar contributions (colour code: green, positive; purple, negative); c) Positive ionic (colour code: blue, positive; orange-yellow, negative); d) Electronegative (colour code: pale red, positive; light green, negative). (For interpretation of the references to colour in this figure legend, the reader is referred to the web version of this article.)

5. Conclusions

The synthesis, inhibition of Hsp90 and assessment of the cytotoxicity of a series of new isoxazolo-fused naphthoquinones and isoquinolinoquinones was carried out.

The available evidence based on the biochemical and cellular effects indicates that the compounds described in this paper represent a novel series of Hsp90 inhibitors. Specific variations of the structure improved the Hsp90 inhibitory effect. In particular, compounds containing an alkylated pyridinium moieties showed high affinity and strong antiproliferative effects. The *in vivo* activity of a representative compound (**7f**) against human epithelial carcinoma A431 model, growing as tumour xenograft in nude mice, supports the therapeutic potential of this novel series of Hsp90 inhibitors.

6. Experimental

6.1. General

All reagents and solvents were reagent grade or were purified by standard methods before use. Melting points were determined in open capillaries. NMR spectra were recorded at 300 MHz. Solvents were routinely distilled prior to use; anhydrous tetrahydrofuran (THF) and ether (Et_2O) were obtained by distillation from sodium–benzophenone ketyl; dry dichloromethane was obtained by distillation from phosphorus pentoxide. All reactions requiring anhydrous conditions were performed under a positive nitrogen flow, and all glassware were oven dried and/or flame dried. Isolation and purification of the compounds were performed by flash column chromatography on silica gel 60 (230–400 mesh). Analytical thin-layer chromatography (TLC) was conducted on TLC plates (silica gel 60 F_{254}, aluminium foil) visualized by UV light.

6.2. General procedure for the cycloaddition reaction

The appropriate quinone (10.5 mmol), triethylamine (100 mg, 0.98 mmol) and 15% aqueous sodium hypochlorite (15 mL) were added to dichloromethane (10 mL), then the appropriate oxime (10.5 mmol) was added dropwise at 0 °C over 15 min. After stirring for 1.5 h, the reaction phases were separated and the aqueous phase was extracted with dichloromethane. The organic phase was dried with Na_2SO_4 and the solvent was removed under reduced pressure. The residue was purified by flash chromatography to give the desired product.

Thus, when not stated otherwise, were prepared the following products:

6.2.1. 3-Phenyl-naphtho[2,3–d]isoxazole-4,9-dione (**3a**)

Purified by flash chromatography. (Eluent CH_2Cl_2). Sticky pale yellow solid. (55%). ^{1}H NMR (DMSO-d_6) δ: 8.27–8.14 (m, 2H), 8.12–8.03 (m, 2H), 7.98–7.88 (m, 2H), 7.69–7.52 (m, 3H). Anal calcd for $C_{17}H_9NO_3$ (275.26): C 74.18, H 3.30, N 5.09. Found: C 74.39, H 3.12, N 5.19.

6.2.2. 3-(4-Methoxyphenyl)-naphtho[2,3–d]isoxazole-4,9-dione (**3b**)

Purified by flash chromatography (Eluent hexane/AcOEt 3:2). Brown solid. (60%). Mp.: 163–164 °C. ^{1}H NMR (DMSO-d_6) δ: 8.28–8.17 (m, 2H), 8.11 (d, 2H, J = 8.5 Hz), 8.03–7.89 (m, 2H), 7.18 (d, 2H, J = 8.5 Hz), 3.88 (s, 3H). Anal calcd for $C_{18}H_{11}NO_4$ (305.28): C 70.82, H 3.63, N 4.59. Found: C 70.56, H 3.79, N 4.41.

6.2.3. 3-(4-Hydroxyphenyl)-naphtho[2,3–d]isoxazole-4,9-dione (**3c**)

Compound **3b** (100 mg, 0.33 mmol) was dissolved in 2 mL of HBr 35% in acetic acid and the solution was refluxed for 5 h. After cooling at room temperature, dichloromethane was added and the organic phase was washed with sodium bicarbonate, water and dried over Na_2SO_4. The solvent was evaporated under reduce pressure to give a crude that was purified by flash chromatography (CH_2Cl_2/CH_3OH, 97.5:2.5) to obtain 80 mg of **3c** as an orange sticky solid (83%). ^{1}H NMR (DMSO-d_6) δ: 10.15 (brs, 1H), 8.25–8.12 (m, 2H), 8.05–7.89 (m, 4H), 7.00–6.90 (m, 2H). Anal calcd for $C_{17}H_9NO_4$ (291.26): C 70.10, H 3.11, N 4.81. Found: C 70.35, H 3.01, N 4.59.

6.2.4. 3-(4-Fluorophenyl)-naphtho[2,3–d]isoxazole-4,9-dione (**3d**)

Purified by flash chromatography (Eluent CH_2Cl_2). Pale yellow solid (31%). Mp.: 166–167 °C. ^{1}H NMR (DMSO-d_6) δ: 8.27–8.08 (m, 4H), 8.02–7.83 (m, 2H), 7.56–7.35 (m, 2H). Anal calcd for $C_{17}H_8FNO_3$ (293.25): C 69.63, H 2.75, N 4.78. Found: C 69.32, H 2.98, N 4.55.

6.2.5. 3-(2-Methoxyphenyl)-naphtho[2,3–d]isoxazole-4,9-dione (**3e**)

Purified by flash chromatography (Eluent CH_2Cl_2). Bright yellow solid (57%). Mp.: 212–214 °C. ^{1}H NMR (DMSO-d_6) δ: 8.23–8.14 (m, 1H), 8.13–8.03 (m, 1H), 7.99–7.90 (m, 2H), 7.66–7.56 (m, 1H), 7.48 (d, 1H, J = 8.0 Hz), 7.26 (d, 1H, J = 8.4 Hz), 7.16–7.07 (m, 1H), 3.76 (s, 3H). Anal calcd for $C_{18}H_{11}NO_4$ (305.28): C 70.82, H 3.63, N 4.59. Found: C 70.66, H 3.91, N 4.39.

6.2.6. 3-(2-Hydroxyphenyl)-naphtho[2,3–d]isoxazole-4,9-dione (**3f**)

Compound **3e** (50 mg, 0.16 mmol) was dissolved in 4 mL of dry dichloromethane at 0 °C and 1 M boron tribromide solution in dichloromethane (200 μL) was added under nitrogen. The mixture was stirred at 0 °C for 1.5 h then at room temperature for 30 min. The solution was diluted with dichloromethane, washed with sodium bicarbonate, dried over Na_2SO_4 and evaporated under reduced pressure. The residue was purified by flash chromatography (CH_2Cl_2) to give 45 mg of **3f** as a yellow solid (93%). Mp.: 190–191 °C. ^{1}H NMR ($CDCl_3$) δ: 9.19 (s, 1H), 8.74 (dd, 1H, J = 8.4, 1.9 Hz), 8.37–8.30 (m, 2H), 7.96–7.85 (m, 2H), 7.53–7.46 (m, 1H), 7.18–7.11 (m, 2H). Anal calcd for $C_{17}H_9NO_4$ (291.26): C 70.10, H 3.11, N 4.81. Found: C 70.29, H 2.98, N 4.67.

6.2.7. 3-(5-Chloro-2,4-dimethoxyphenyl)-naphtho[2,3–d]isoxazole-4,9-dione (**3g**)

Purified by flash chromatography (Eluent hexane/AcOEt 3:2). Dark yellow sticky solid (75%). ^{1}H NMR ($CDCl_3$) δ: 8.34–8.25 (m, 1H), 8.24–8.12 (m, 1H), 7.92–7.73 (m, 2H), 7.56 (s, 1H), 6.66 (s, 1H), 4.03 (s, 3H), 3.85 (s, 3H). Anal calcd for $C_{19}H_{12}ClNO_5$ (369.76): C 61.72, H, 3.27, N 3.79. Found: C 61.94, H, 3.08, N 3.85.

6.2.8. 3-(5-Chloro-2-hydroxy-4-methoxyphenyl)-naphtho[2,3–d]isoxazole-4,9-dione (**3h**)

Compound **3g** (100 mg, 0.27 mmol) was dissolved in 8 mL of dry dichloromethane at 0 °C and 1 M boron tribromide in dichloromethane (0.5 mL) was added under nitrogen. The mixture was stirred at 0 °C for 1.5 h then at room temperature for 1 h. The solution was diluted with dichloromethane, washed with sodium bicarbonate, dried over Na_2SO_4 and evaporated under reduced pressure to give 90 mg of **3h** as a yellow solid (94%). Mp.: 205–206 °C. ^{1}H NMR (DMSO-d_6) δ: 10.48 (brs, 1H), 8.21–8.15 (m, 1H), 8.12–8.05 (m, 1H), 7.98–7.89 (m, 2H), 7.49 (s, 1H), 6.74 (s, 1H), 3.90 (s, 3H). Anal calcd for $C_{18}H_{10}ClNO_5$ (355.73): C 60.77, H 2.83, N 3.94. Found: C 60.58, H 2.99, N 3.79.

6.2.9. 3-(5-Chloro-2,4-dihydroxyphenyl)-naphtho[2,3–d]isoxazole-4,9-dione (**3i**)

Compound **3h** (140 mg, 0.39 mmol) was dissolved in 15 mL of HBr 35% in acetic acid and the solution was refluxed for 48 h. After

cooling at room temperature, dichloromethane was added and the organic phase was washed with sodium bicarbonate, water and dried over Na_2SO_4. The solvent was evaporated under reduced pressure to give a crude that was purified by flash chromatography (CH_2Cl_2/acetone 99:1) to obtain 30 mg of **3i** as a yellow solid (23%). Mp.: 199–200 °C ^{1}H NMR ($CDCl_3$) δ: 10.07 (brs, 1H), 9.05 (brs, 1H), 8.44–8.25 (m, 2H), 8.00–7.84 (m, 3H), 6.36 (s, 1H). Anal calcd for $C_{17}H_8ClNO_5$ (341.70): C 59.75, H 2.36, N 4.10. Found C 59.53, H 2.56, N 4.21.

*6.2.10. 4-{2-[4-(4,9-dioxo-4,9-dihydronaptho[2,3–d]isoxazol-3-yl)-phenoxy]-ethyl}-morpholin-4-ium chloride (**3k**)*

Purified by flash chromatography (Eluent CH_2Cl_2/CH_3OH 95:5). The product was dissolved in dichloromethane (5 mL) and treated with conc. HCl in 1,4-dioxane until pH = 2. The solid was filtered and washed with diethyl ether to give a yellow solid (52%). Mp.: 240 °C. ^{1}H NMR (DMSO-d_6) δ: 10.70 (brs, 1H), 8.28–8.09 (m, 4H), 8.07–7.91 (m, 2H), 7.25 (d, 2H, J = 8.5 Hz), 4.65–4.48 (m, 2H), 4.12–3.95 (m, 2H), 3.90–3.74 (m, 2H), 3.70–3.49 (m, 4H), 3.31–3.02 (m, 2H). Anal calcd for $C_{23}H_{21}ClN_2O_5$ (440.88): C 62.66, H 4.80, N 6.35. Found: C 62.79, H 4.65, N 6.21.

*6.2.11. 3-(1H-indol-5-yl)-naphtho[2,3–d]isoxazole-4,9-dione (**3l**)*

Purified by flash chromatography (Eluent hexane/AcOEt 2:1). Sticky solid (35%). ^{1}H NMR $(CD_3)_2CO$ δ: 8.58 (s, 1H), 8.35–8.21 (m, 2H), 8.06–7.87 (m, 3H), 7.61 (d, 1H, J = 8.6 Hz), 7.51–7.44 (m, 1H), 6.72–6.63 (m, 1H). Anal calcd for $C_{19}H_{10}N_2O_3$ (314.29): C 72.61, H 3.21, N 8.91. Found: C 72.87, H 3.05, N 8.65.

*6.2.12. 3-Styryl-naphtho[2,3–d]isoxazole-4,9-dione (**3m**)*

Purified by flash chromatography (Eluent hexane/AcOEt 4:1). Bright yellow sticky solid (40%). ^{1}H NMR ($CDCl_3$) δ: 8.38–8.28 (m, 2H), 8.24 (d, 1H, J = 16.2 Hz), 7.95–7.80 (m, 2H), 7.73–7.62 (m, 2H), 7.52–7.36 (m, 4H). Anal calcd for $C_{19}H_{11}NO_3$ (301.30): C 75.74, H 3.68, N 4.65. Found: C 75.48, H 3.89, N 4.45.

*6.2.13. 3-Pyridin-4-yl-naphtho[2,3–d]isoxazole-4,9-dione (**3n**)*

Purified by flash chromatography (Eluent CH_2Cl_2/CH_3OH 20:1). Yellow solid (26%). Mp.: 220 °C. ^{1}H NMR (DMSO-d_6) δ: 8.88 (d, 2H, J = 6.1 Hz), 8.32–8.17 (m, 2H), 8.08 (d, 2H, J = 6.1 Hz), 8.06–7.93 (m, 2H). Anal calcd for $C_{16}H_8N_2O_3$ (276.25): C 69.57, H 2.92, N 10.14. Found: C 69.39, H 3.09, N 10.34.

*6.2.14. 3-Pyridin-3-yl-naphtho[2,3–d]isoxazole-4,9-dione (**3o**)*

Purified by flash chromatography (Eluent CH_2Cl_2/CH_3OH 97.5: 2.5). Light yellow solid (91%). Mp.: 188–189 °C. ^{1}H NMR (DMSO-d_6) δ: 9.21 (s, 1H), 8.89–8.80 (m, 1H), 8.51–8.40 (m, 1H), 8.29–8.02 (m, 2H), 8.08–7.91 (m, 2H), 7.73–7.62 (m, 1H). Anal calcd for $C_{16}H_8N_2O_3$ (276.25): C 69.57, H 2.92, N 10.14. Found: C 69.69, H 2.75, N 10.27.

*6.2.15. 3-Pyridin-2-yl-naphtho[2,3–d]isoxazole-4,9-dione (**3p**)*

Purified by flash chromatography (Eluent CH_2Cl_2/CH_3OH 97.5: 2.5). Yellow solid (28%). Mp.: 170–171 °C. ^{1}H NMR (DMSO-d_6) δ: 8.88–8.79 (m, 1H), 8.28–8.07 (m, 4H), 8.03–7.92 (m, 2H), 7.76–7.60 (m, 1H). Anal calcd for $C_{16}H_8N_2O_3$ (276.25): C 69.57, H 2.92, N 10.14. Found: C 69.78, H 2.72, N 10.29.

*6.2.16. Acetic acid 3-(4-fluorophenyl)-4,9-dioxo-4,9-dihydronaphtho[2,3–d]isoxazol-5-yl ester (**6a**)*

Purified by flash chromatography (Eluent CH_2Cl_2/CH_3OH 40:1) Yellow solid (57%). Mp.: 191–192 °C. ^{1}H NMR ($CDCl_3$) δ: 8.27 (dd, 1H, J = 7.8, 1.1 Hz), 8.14–8.05 (m, 2H), 7.85 (dd, 1H, J = 7.8, 7.8 Hz), 7.50 (dd, 1H, J = 7.82, 1.12 Hz), 7.28–7.18 (m, 2H), 2.47 (s, 3H). Anal calcd for $C_{19}H_{10}FNO_5$ (351.28): C 64.96, H 2.87, N 3.99. Found: C 65.09, H 2.67, N 4.11.

*6.2.17. 3-(4-Fluorophenyl)-5-hydroxynaphtho[2,3–d]isoxazole-4,9-dione (**6b**)*

Compound **6a** (50 mg, 0.14 mmol) was dissolved in 7 mL of methanol and K_2CO_3 (50 mg, 0.36 mmol) in 3 mL of water was added under nitrogen. After stirring for 40 min at room temperature, the solution was poured into water and acidified with diluted acetic acid. The solution was extracted with dichloromethane and the organic phase was washed with water, dried over Na_2SO_4 and evaporated under reduced pressure. The residue was purified by flash chromatography (CH_2Cl_2) to give 35 mg of **6b** (80%). Orange solid Mp.: 208–209 °C. ^{1}H NMR ($CDCl_3$) δ: 12.20 (brs, 1H), 8.20–8.12 (m, 2H), 7.87 (d, 1H, J = 8.2 Hz), 7.75–7.68 (m, 1H), 7.40 (d, 1H, J = 8.2 Hz), 7.30–7.21 (m, 2H). Anal calcd for $C_{17}H_8FNO_4$ (309.25): C 66.03, H 2.61, N 4.53. Found: C 66.24, H 2.41, N 4.29.

*6.2.18. 5-Methoxy-3-pyridin-4-yl-naphtho[2,3–d]isoxazole-4,9-dione (**6c**)*

Purified by flash chromatography (Eluent CH_2Cl_2/CH_3OH 96:4). Yellow solid (35%). Mp.: 214–215 °C. ^{1}H NMR ($CDCl_3$) δ: 8.81 (d, 2H, J = 6.1 Hz), 8.07 (d, 2H, J = 6.1 Hz), 7.96 (d, 1H, J = 8.0 Hz), 7.78 (dd, 1H, J = 8.4 and 8.0 Hz), 7.46 (d, 1H, J = 8.4 Hz), 4.06 (s, 3H). Anal. Calcd. for $C_{17}H_{10}N_2O_4$ (306.27): C 66.67, H 3.29, N 9.15. Found: C 66.99, H 3.01, N 9.15.

*6.2.19. Acetic acid 4,9-dioxo-3-pyridin-4-yl-4,9-dihydro-naphtho [2,3–d]isoxazol-5-yl ester (**6d**)*

Purified by flash chromatography (Eluent CH_2Cl_2/CH_3OH 97:3). Brown solid (29%). Mp.: 151–152 °C. ^{1}H NMR ($CDCl_3$) δ: 8.95–8.74 (m, 2H), 8.30 (d, 1H, J = 8.0 Hz), 8.03–7.96 (m, 2H), 7.89–7.80 (m, 1H), 7.50 (d, 1H, J = 8.4 Hz), 2.46 (s, 3H). Anal calcd for $C_{18}H_{10}N_2O_5$ (334.28): C 64.67, H 3.02, N 8.38. Found C 64.98, H 2.98, N 8.49.

*6.2.20. 5-Hydroxy-3-pyridin-4-yl-naphtho[2,3–d]isoxazole-4,9-dione (**6e**)*

Compound **6d** (120 mg, 0.36 mmol) was dissolved in 10 mL of methanol and K_2CO_3 (360 mg, 2.6 mmol) in 7 mL of water was added under nitrogen. After stirring for 30 min at room temperature, the solution was poured into water and acidified with diluted acetic acid. The solution was extracted with dichloromethane and the organic phase was washed with water, dried over Na_2SO_4 and evaporated under reduced pressure. The residue was purified by flash chromatography (CH_2Cl_2/hexane, 50:50) to give 100 mg of **6e** as an orange solid (95%). Mp.: 210–211 °C. ^{1}H NMR ($CDCl_3$) δ: 12.16 (brs, 1H), 8.84(d, 2H, J = 6.1 Hz), 8.05 (d, 2H, J = 6.1 Hz), 7.86 (d, 1H, J = 7.8 Hz), 7.72 (dd, 1H, J = 8.2, 7.8 Hz), 7.40 (d, 1H, J = 8.2 Hz). Anal calcd for $C_{16}H_8N_2O_4$ (292.25): C 65.76, H 2.76, N 9.59. Found: C 65.56, H 2.98, N 9.72.

*6.2.21. 3-(4-Fluorophenyl)-1-oxa-2,6-diazacyclopenta[b] naphthalene-4,9-dione (**10a**)*

Purified by flash chromatography (Eluent CH_2Cl_2/CH_3OH 96:4). (27%). ^{1}H NMR ($CDCl_3$) δ: 9.56 (s, 1H), 9.22 (d, 1H, J = 4.8 Hz), 8.30–8.22 (m, 2H), 8.09 (d, 1H, J = 4.8 Hz), 7.35–7.27 (m, 2H). Anal calcd for $C_{16}H_7FN_2O_3$ (294.24): C 65.31, H 2.40, N 9.52. Found: C 65.54, H 2.63, N 9.28.

*6.2.22. 3-(4-Methoxyphenyl)-1-oxa-2,6-diaza-cyclopenta[b] naphthalene-4,9-dione (**10b**)*

Purified by flash chromatography (Eluent CH_2Cl_2/CH_3OH 97.5:2.5) Yellow solid (30%). Mp.: 182–183 °C. ^{1}H NMR ($CDCl_3$) δ: 9.56 (s, 1H), 9.22 (d, 1H, J = 8.3 Hz), 8.27–8.12 (m, 2H), 8.10–8.03 (m, 1H), 7.05 (d, 2H, J = 8.3 Hz), 3.91 (s, 3H). Anal calcd for $C_{17}H_{10}N_2O_4$ (306.27): C 66.67, H 3.29, N 9.15. Found: C 66.41, H 3.50, N 9.28.

*6.2.23. 4-{2-[4-(4,9-dioxo-4,9-dihydro-1-oxa-2,6-diazacyclopenta [b]naphthalen-3-yl)-phenoxy]-ethyl}-morpholin-4-ium chloride (**10c**)*

Purified by flash chromatography (Eluent CH_2Cl_2/CH_3OH 95:5). The product was dissolved in dichloromethane (5 mL) and treated with conc. HCl in 1,4-dioxane until pH = 2. The solid was filtered and washed with diethyl ether (19%). Mp.: 194–195 °C. ^{1}H NMR (DMSO-d_6) δ: 11.20 (brs, 1H), 9.41 (s, 1H), 9.24 (d, 1H, J = 4.8 Hz), 8.21–8.02 (m, 3H), 7.29 (d, 2H, J = 8.5 Hz), 4.69–4.52 (m, 2H), 4.20–3.20 (m, 10H). Anal calcd for $C_{22}H_{20}ClN_3O_5$ (441.86): C 59.80, H 4.56, N 9.51. Found: C 59.59, H 4.68, N 9.66.

*6.2.24. 3-Pyridin-4-yl-1-oxa-2,6-diaza-cyclopenta[b]naphthalene-4,9-dione (**10d**)*

Purified by flash chromatography (Eluent CH_2Cl_2/CH_3OH 20:1) (20%). ^{1}H NMR ($CDCl_3$) δ: 9.58 (s, 1H), 9.23 (d, 1H, J = 4.8 Hz), 8.89 (d, 2H, J = 5.1 Hz), 8.27–8.17 (d, 2H, J = 5.1 Hz), 8.08 (d, 1H, J = 4.8 Hz). Anal calcd for $C_{15}H_7N_3O_3$ (277.23): C 64.98, H 2.54, N 15.16. Found: C 64.71, H 2.76, N 15.28.

6.3. General procedure for the alkylation reaction

The appropriate 3-pyridyl derivative (0.1 mmol) was dissolved in 1 mL of DMSO and benzyl bromide (0.33 mmol) was added. The mixture was stirred at room temperature overnight under nitrogen. After cooling diethyl ether was added, the solid was filtered, washed with diethyl ether and crystallized.

Thus, when not stated otherwise, were prepared the following products:

*6.3.1. 1-Benzyl-4-(5-methoxy-4,9-dioxo-4,9-dihydronaphtho [2,3–d]isoxazol-3-yl)-pyridinium bromide (**7a**)*

Yellow solid (64%). Mp.: 216–218 °C (from methanol/diethyl ether). ^{1}H NMR (DMSO-d_6) δ: 9.44 (d, 2H, J = 5.9 Hz), 8.80 (d, 2H, J = 5.9 Hz), 7.99–7.88 (m, 2H), 7.78–7.69 (m, 1H), 7.67–7.57 (m, 2H), 7.56–7.42 (m, 3H), 5.99 (s, 2H), 3.98 (s, 3H). Anal calcd for $C_{24}H_{17}BrN_2O_4$ (477.31): C 60.39, H 3.59, N 5.87. Found: C 60.61, H 3.32, N 5.65.

*6.3.2. 4-(5-Acetoxy-4,9-dioxo-4,9-dihydronaphtho[2,3–d]isoxazol-3-yl)-1-benzyl-pyridinium bromide (**7b**)*

Yellow solid (97%). Mp.: 203–204 °C (from methanol). ^{1}H NMR (DMSO-d_6) δ: 9.45 (d, 2H, J = 5.9 Hz), 8.77 (d, 2H, J = 5.9 Hz), 8.25–8.17 (m, 1H), 8.09–7.99 (m, 1H), 7.79–7.70 (m, 1H), 7.67–7.59 (m, 2H), 7.54–7.43 (m, 3H), 5.98 (s, 2H), 2.39 (s, 3H). Anal calcd for $C_{25}H_{17}BrN_2O_5$ (505.32): C 59.42, H 3.39, N. 5.54. Found: C 59.63, H 3.54, N. 5.40.

*6.3.3. 1-Benzyl-4-(5-hydroxy-4,9-dioxo-4,9-dihydronaphtho [2,3–d]isoxazol-3-yl)-pyridinium bromide (**7c**)*

Yellow solid (65%). Mp.: 198–199 °C (from methanol/diethyl ether). ^{1}H NMR (DMSO-d_6) δ: 11.79 (s, 1H), 9.47 (d, 2H, J = 6.5 Hz), 8.83 (d, 2H, J = 6.5 Hz), 7.90–7.77 (m, 2H), 7.67–7.58 (m, 2H), 7.56–7.43 (m, 4H), 6.01 (s, 2H). Anal calcd for $C_{23}H_{15}BrN_2O_4$ (463.28): C 59.63, H 3.26, N 6.05. Found: C 59.38, H 3.48, N 6.25.

*6.3.4. 4-(4,9-Dioxo-4,9-dihydronaphtho[2,3–d]isoxazol-3-yl)-1-methylpyridinium iodide (**7d**)*

Compound **3n** (30 mg, 0.1 mmol) was dissolved in 1 mL of methanol and iodomethane (1 mL) was added. The mixture was stirred at room temperature overnight then the solvent was evaporated under reduce pressure. The crude was purified by crystallization with methanol/dichloromethane to give 15 mg of **7d** as a yellow solid (36%). Mp.: 210–211 °C. ^{1}H NMR (DMSO-d_6) δ: 9.25 (d, 2H, J = 6.0 Hz), 8.81 (d, 2H, J = 6.0 Hz), 8.31–8.17 (m, 2H), 8.10–7.94 (m, 2H), 4.49 (s, 3H). Anal calcd for $C_{17}H_{11}IN_2O_3$ (418.19): C 48.83, H 2.65, N 6.70. Found: C 48.55, H 2.91, N 6.52.

*6.3.5. 4-(4,9-Dioxo-4,9-dihydro-naphtho[2,3–d]isoxazol-3-yl)-1-(pyrazin-2-yl)methyl-pyridinium bromide (**7e**)*

Compound **3n** (50 mg, 0.18 mmol) was dissolved in 1.5 ml of DMSO and 2-bromomethylpyrazine (50 mg, 0.28 mmol) was added. After having stirred for 72 h at room temperature under nitrogen, the solution was poured into water and extracted with dichloromethane. The organic phase was dried and evaporated under reduced pressure. The residue was purified by crystallization with methanol/diethyl ether to give 30 mg of **7e**. as a yellow solid (37%) Mp.: 170–171 °C. ^{1}H NMR (DMSO-d_6) δ: 9.45 (d, 2H, J = 5.9 Hz), 9.05 (s, 1H), 8.92 (d, 2H, J = 5.9 Hz), 8.86 (s, 1H), 8.81 (s, 1H), 8.31–8.20 (m, 2H), 8.12–8.00 (m, 2H), 6.28 (s, 2H). Anal calcd for $C_{21}H_{13}BrN_4O_3$ (449.26): C 56.14, H 2.92, N 12.47. Found: C 56.38, H 2.69, N 12.30.

*6.3.6. 1-Benzyl-4-(4,9-dioxo-4,9-dihydro-naphtho[2,3–d]isoxazol-3-yl)-pyridinium bromide (**7f**)*

Yellow solid (56%). Mp.: 206 °C. ^{1}H NMR (DMSO-d_6) δ: 9.51 (d, 2H, J = 6.1 Hz), 8.89 (d, 2H, J = 6.1 Hz), 8.35–8.18 (m, 2H), 8.11–7.96 (m, 2H), 7.78–7.59 (m, 2H), 7.55–7.40 (m, 3H), 6.01 (s, 2H). Anal calcd for $C_{23}H_{15}BrN_2O_3$ (447.28): C 61.76, H 3.38, N. 6.26. Found: C 61.57, H 3.61, N. 6.01.

*6.3.7. 1-Benzyl-2-(4,9-dioxo-4,9-dihydro-naphtho[2,3–d]isoxazol-3-yl)-pyridinium bromide (**7g**)*

Purified by flash chromatography (CH_2Cl_2/CH_3OH, 4:1). Sticky solid (37%). ^{1}H NMR (DMSO-d_6) δ: 8.79–8.70 (m, 1H), 8.57–8.42 (m, 1H), 8.03–7.95 (m, 1H), 7.93–7.81 (m, 3H), 8.80–7.70 (m, 1H), 7.69–7.60 (m, 1H), 7.46–7.25 (m, 5H), 5.69 (s, 2H). Anal calcd for $C_{23}H_{15}BrN_2O_3$ (447.28): C 61.76, H 3.38, N. 6.26. Found: C 61.56, H 3.65, N. 6.45.

*6.3.8. 1-Benzyl-3-(4,9-dioxo-4,9-dihydro-naphtho[2,3–d]isoxazol-3-yl)-pyridinium bromide (**7h**)*

Yellow solid. (60%). Mp.: 184–185 °C (from methanol/diethyl ether). ^{1}H NMR (DMSO-d_6) δ: 9.98 (s, 1H), 9.52–9.41 (m, 1H), 9.35–9.24 (m, 1H), 8.53–8.39 (m, 1H), 8.30–8.15 (m, 2H), 8.09–7.98 (m, 2H), 7.75–7.62 (m, 2H), 7.58–7.40 (m, 3H), 6.65 (s, 2H). Anal calcd for $C_{23}H_{15}BrN_2O_3$ (447.28): C 61.76, H 3.38, N. 6.26. Found: C 61.91, H 3.11, N. 6.13.

*6.3.9. 3-(4,9-Dioxo-4,9-dihydro-naphtho[2,3–d]isoxazol-3-yl)-1-pyrazin-2-ylmethyl-pyridinium bromide (**7i**)*

Compound **3o** (50 mg, 0.18 mmol) was dissolved in 1 mL of DMSO and 2-bromomethylpyrazine (50 mg, 0.29 mmol) was added. The mixture was stirred at room temperature for 72 h under nitrogen. After cooling diethyl ether was added, the solid was filtered and purified by crystallization from methanol/diethyl ether to give 58 mg of **7i**. as a brown solid (72%). Mp.: 178–179 °C. ^{1}H NMR (DMSO-d_6) δ: 9.94 (s, 1H), 9.51–9.31 (m, 2H), 9.02 (s, 1H), 8.80–8.63 (m, 2H), 8.60–8.47 (m, 1H), 8.33–8.16 (m, 2H), 8.10–7.91 (m, 2H), 6.29 (s, 2H). Anal calcd for $C_{21}H_{13}BrN_4O_3$ (449.26): C 56.14, H 2.92, N 12.47. Found: C 55.97, H 3.09, N 12.11.

*6.4. Acetic acid 9-acetoxy-3-(4-methoxyphenyl)-4,9-dihydronaphtho[2,3–d]isoxazol-4-yl ester (**8a**)*

Compound **3b** (90 mg, 0.29 mmol), zinc powder (30 mg, 0.45 mmol) and triethylamine (1.4 g, 14 mmol) in 4 mL of acetic anhydride were refluxed for 3 h. After cooling to room temperature, the solution was poured into water and extracted with CH_2Cl_2. The solvent was evaporated under reduced pressure and the residue

was purified by flash chromatography (CH_2Cl_2) to give 60 mg of **8a** (53%). Mp.: 154–155 °C. ^{1}H NMR ($CDCl_3$) δ: 8.05 (d, 1H, $J = 9.3$ Hz), 7.99 (d, 1H, $J = 8.9$ Hz), 7.77 (d, 2H, $J = 8.2$ Hz), 7.70–7.66 (m, 1H), 7.56–7.53 (m, 1H), 7.09 (d, 2H, $J = 8.2$ Hz), 3.93 (s, 3H), 2.62 (s, 3H), 2.10 (s, 3H). Anal calcd for $C_{22}H_{19}NO_6$ (393.39): C 67.17, H 4.87, N 3.56. Found: C 67.39, H 4.65, N 3.40.

6.5. Acetic acid 9-acetoxy-3-(4-fluorophenyl)-4,9-dihydro-naphtho [2,3–d]isoxazol-4-yl ester (**8b**)

Compound **3d** (90 mg, 0.25 mmol), zinc powder (30 mg, 0.45 mmol) and triethylamine (1.4 g, 14 mmol) in 4 mL of acetic anhydride were refluxed for 2 h. After cooling to room temperature, the solution was poured into water and extracted with CH_2Cl_2. The solvent was evaporated under reduced pressure and the residue was purified by flash chromatography (CH_2Cl_2) to give 95 mg of **8b**. (100%). ^{1}H NMR ($CDCl_3$) δ: 8.09–7.94 (m, 2H), 7.88–7.78 (m, 2H), δ 7.71–7.61 (m, 1H), 7.59–7.48 (m, 1H), 7.32–7.20 (m, 2H), 2.60 (s, 3H), 2.09 (s, 3H). Anal calcd for $C_{21}H_{16}FNO_5$ (381.35): C 66.14, H 4.23, N 3.67. Found C 66.34, H 4.01, N 3.51.

6.6. Quality of the pharmacophoric hypotheses

The quality of each pharmacophore was first measured in three ways based on the alignments to the input structures: (1) the alignment score, which is the root-mean-squared deviation (rmsd) in the site-point positions; (2) the vector score, which is the average cosine of the angles formed by corresponding pairs of vector features (acceptors, donors and aromatic rings) in the aligned structures; (3) a volume score based on the overlap of van der Waals models of the non-hydrogen atoms in each pair of structures. For details, see Dixon et al. [36].

6.7. Computational details

All molecules investigated in this study were built with the Maestro 9.1 graphical interface [38] Each structure was subsequently minimized with the OPLS_2005 force field, a constant dielectric of 1.0 and an implicit solvation treatment using MacroModel 9.8 [39]. Conformational sampling was carried out using the same settings of minimization with minimum atom deviation of 0.5 Å. The maximum relative energy difference was set to 2.0 kcal/mol. Pharmacophore development, site-point superpositions, vector characteristics alignment, molecular volume overlap, penalty scoring, and QSAR model building were carried out using Phase 3.2 [40]. All calculations were performed in Maestro 9.1.

Phase QSAR models do not use internal cross-validation techniques, but rather use distinct training and test sets. However, the use of leave-*n*-out techniques are useful for assessing the stability of the model to changes in the training set. In Phase QSAR models, leave-*n*-out models were built, and the.

R^2 value was computed between the leave-*n*-out predictions and the predictions from the model built on the full training set. This value was reported as the stability value. Models with high stability (maximum value = 1) were preferred because they were not overly dependent on any particular training set.

6.8. Biological activity

6.8.1. Cell lines and culture conditions

The epithelial carcinoma cell line A431 and the non-small cell lung carcinoma cell line NCI-H460 were routinely grown in RPMI 1640 (Lonza, Vierviers, Belgium), supplemented with 10% (v/v) heat-inactivated foetal bovine serum (GIBCO, Invitrogen, Paisley, UK). The human peritoneal mesothelioma cell line STO was kindly provided by Dr. N. Zaffaroni (IRCCS Istituto Nazionale Tumori, Milan) and grown in 50/50 DMEM-Ham's F12 medium (Lonza, Vierviers, Belgium), supplemented with 10% (v/v) heat-inactivated foetal bovine serum and 2 mM L-glutamine (L-Gln). All cell lines were maintained at 37 °C in a 5%/95% CO_2/air atmosphere.

6.8.2. Drugs and treatment conditions

All the compounds tested were freshly prepared dissolving powder in dimethylsulfoxide (DMSO) (BDH Prolabo, Milan, Italy) and following dilution in culture medium. Cells were incubated with drugs for 6, 24 or 72 h (depending on the assay), at 37 °C in culture medium supplemented with 10% (v/v) heat-inactivated foetal bovine serum; drug concentrations used for each assay are reported in Legends to Figures.

6.8.3. Fluorescence polarization assay

GM-FITC Geldanamycin- fluorescein-5-isothiocyanate (working concentration: 1–400 nM), supplied by *Invivogen (06C23-MT, California 92192, USA)*, was previously dissolved in DMSO to obtain 10 mM stock solutions and kept at −20 °C until use. Hsp90, purchased from (*Stressgen cat. No. SPP-776, Victoria BC, Canada)*, was previously dissolved in assay buffer (HFB) to form 2.2 μM stock solutions and kept at −80 °C until use.

The compounds were previously dissolved in DMSO to obtain stock solutions and kept at −20 °C. The day of experiment, the compounds were prepared by serial dilutions in assay buffer (HFB) containing 20 mM HEPES (K) pH 7.3, 50 mM KCl, 5 mM $MgCl_2$, 20 mM Na_2MoO_4 and 0.01% NP40. Before each use, 0.1 mg/ml Bovine Gamma globulin and 2 mM DTT were freshly added.

Fluorescence Polarization (FP) was performed in Opti-Plate™-96F well plates *(Perkin Elmer, Zaventem, Belgium)* using a plate reader (*Wallac Envision 2101 multilabel reader, Perkin Elmer, Zaventem, Belgium)*. To evaluate the binding affinity of the molecules, 50 μl of the GM-FTC solution (5 nM) were added to 30 nM of Hsp90 in the presence of 5 μl of the test compounds at increasing concentrations. The plate was mixed on a shaker at 4 °C for 4 h, and the FP values in mP (millipolarization units) were recorded. The IC_{50} values were calculated as the inhibitor concentration where 50% of the tracer is displaced; each data point is the result of the average of triplicate wells, and was determined from a plot using nonlinear least-squares analysis. Curve fitting was performed using *Prism GraphPad* software program (*GraphPad software, Inc., San Diego, CA)*.

6.8.4. Protein expression analysis

Total cell lysates were prepared rinsing cells twice with ice-cold PBS supplemented with 0.1 mM sodium orthovanadate, then lysing them in hot sample buffer as previously described [41]. After determination of protein concentration (BCA Protein Assay Reagent, Pierce, Thermo Fisher Scientific Inc., Rockford, IL, USA), whole-cell extracts were separated by SDS polyacrylamide gel electrophoresis (PAGE) and transferred onto nitrocellulose membranes. Detection of proteins was accomplished using horseradish peroxidase-conjugated secondary antibodies and a chemiluminescence reagent purchased through Amersham Biosciences (Rockford, IL). For quantification of signals, blots were also subjected to densitometry analysis.

Primary antibodies used in this study are: anti-Raf-1 and anti-Cdk4 (Santa Cruz Biotechnology Inc., CA, USA), anti-EGFR (Upstate Biotechnology, Millipore Corporate, Billerica, MA, USA), anti-Survivin (Abcam, Cambridge, UK), anti-Akt (Transduction Laboratories, Lexington, USA), anti-HSP70 (BRM-22) and anti-Actin (Sigma Chemical Co., St. Louis, MO, USA).

6.8.5. Animals

Experiments were carried out using female athymic Swiss nude mice, 8–10 weeks old (Charles River, Calco, Italy). Mice were maintained in laminar flow rooms keeping temperature and humidity constant. Mice had free access to food and water. Experiments were approved by the Ethics Committee for Animal Experimentation of the Istituto Nazionale Tumori of Milan according to institutional guidelines.

Acknowledgements

We thank Mr. Silvio Zavatto for the excellent technical assistance. This work was supported by grants from Sigma-Tau Research, Switzerland S.A., P.O. Box 1823 Via Motta 2a - CH-6850 Mendrisio, Switzerland, Tel.: (+41)091640.4050.

Appendix A. Supplementary data

Supplementary data associated with this article can be found, in the online version, at doi:10.1016/j.ejmech.2012.03.036.

References

[1] C. Prodromou, S.M. Roe, R. O'Brien, J.E. Ladbury, P.W. Piper, L.H. Pearl, Cell 90 (1997) 65–75.
[2] L. Whitesell, S.L. Lindquist, Nat. Rev. Cancer 5 (2005) 761–772.
[3] (a) K. Richter, J. Buchner, Structure 19 (2011) 445–446;
(b) S.K. Calderwood, J. Gong, J. Cell. Biochem. (2011). doi:10.1002/jcb.23461.
[4] A.E. Kabakov, V.A. Kudryavtsev, Curr. Top. Pharmacol. 14 (2010) 89–102.
[5] A. Donnelly, B.S.J. Blagg, Curr. Med. Chem. 15 (2008) 2702–2717.
[6] Y.L. Janin, Drug Discov. Today 15 (2010) 342–343.
[7] L. Neckers, Trends Mol. Med. 8 (2002) S55–S61.
[8] Y.L. Janin, J. Med. Chem. 48 (2005) 7503–7512.
[9] M.J. Drysdale, P.A. Brough, Drug Discov. Today 13 (2008) 38–43.
[10] T. Taldone, A. Gozman, R. Maharaj, G. Chiosis, Curr. Opin. Pharmacol. 8 (2008) 370–374.
[11] (a) M.A. Biamonte, R. Van de Water, J.W. Arndt, R.H. Scannevin, D. Perret, W.-C. Lee, J. Med. Chem. 53 (2010) 3–17;
(b) S. Messaoudi, J.F. Peyrat, J.D. Brion, M. Alami, Expert Opin. Ther. Pat 21 (2011) 1501–1542.
[12] M.A. Colucci, C.J. Moody, G.D. Couch, Org. Biomol. Chem. 6 (2008) 637–656.
[13] M.K. Hadden, S.A. Hill, J. Davenport, R.L. Matts, B.S.J. Blagg, Bioorg. Med. Chem. 17 (2009) 634–640.
[14] (a) A. Gopalsamy, M. Shi, J. Golas, E. Vogan, J. Jacob, M. Johnson, F. Lee, R. Nilakantan, R. Petersen, K. Svenson, R. Chopra, M.S. Tam, Y. Wen, J. Ellingboe, K. Arndt, F. Boschelli, J. Med. Chem. 51 (2008) 373–375;
(b) P.A. Brough, W. Aherne, X. Barril, J. Borgognoni, K. Boxall, J.E. Cansfield, K.-M.J. Cheung, I. Collins, N.G.M. Davies, M.J. Drysdale, B. Dymock, S.A. Eccles, H. Finch, A. Fink, A. Hayes, R. Howes, R.E. Hubbard, K. James, A.M. Jordan, A. Lockie, V. Martins, A. Massey, T.P. Matthews, E. McDonald, C.J. Northfield, L.H. Pearl, C. Prodromou, S. Ray, F.I. Raynaud, S.D. Roughley, S.Y. Sharp, A. Surgenor, D.L. Walmsley, P. Webb, M. Wood, P. Workman, L. Wright, J. Med. Chem. 51 (2008) 196–218;
(c) R. Baruchello, D. Simoni, G. Grisolia, G. Barbato, P. Marchetti, R. Rondanin, S. Mangiola, G. Giannini, T. Brunetti, D. Alloatti, G. Gallo, A. Ciacci, L. Vesci, M. Castorina, F.M. Milazzo, M.L. Cervoni, M.B. Guglielmi, M. Barbarino, R. Fodera, C. Pisano, W. Cabri, J. Med. Chem. 54 (2011) 8592–8604.
[15] T. Taldone, W. Sun, G. Chiosis, Bioorg. Med. Chem. 17 (2009) 2225–2235.
[16] C. Grundmann, P. Grünanger, Nitrile Oxides, Springer Verlag, Berlin, 1971.
[17] (a) A. Quilico, G. Stagno D'Alcontres, Gazz. Chim. Ital 80 (1950) 140–150;
(b) S. Morrocchi, A. Quilico, A. Ricca, A. Selva, Gazz. Chim. Ital 98 (1968) 891–906;
(c) T. Matsuura, J.W. Bode, Y. Hachisu, K. Suzuki, Synlett (2003) 1746–1748;
(d) N. Ben Hamadi, M. Msaddek, Heterocycl. Comm. 12 (2006) 457–462.
[18] (a) R. Fusco, S. Maiorana, P. Del Buttero, E. Licandro, A. Alemagna, Chim. e Ind. (Milan) 63 (1981) 401–404;
(b) M.P. Fernandez, B. Gonzalez, M. Pardo, J.L. Soto, Anal. Quim 90 (1994) 477–482;
(c) G. Brahmeshwari, V.R. Rao, T.V.P. Rao, Indian J. Chem. 34B (1995) 139–140;
(d) F. Farina, M.V. Martin, M. Munoz, M.C. Paredes, R. Rodriguez, Heterocycles 40 (1995) 413–424.
[19] G.A. Lee, Synthesis (1982) 508–509.
[20] J.L. Stevens, T.D. Welton, J.P. Deville, V. Behar, Tetr. Lett. 44 (2003) 8901–8903.
[21] Y. Kitani, A. Morita, T. Kumamoto, T. Ishikawa, Helv. Chim. Acta 85 (2002) 1186–1195.
[22] (a) R.W. Rickards, J.M. Rothschild, A.C. Willis, M.M. de Chazal, J. Kirk, K. Kirk, K.J. Saliba, G.D. Smith, Tetrahedron 55 (1999) 13513–13520;
(b) P.H. Bernardo, C.L.L. Chai, M. Le Guen, G.D. Smith, P.H. Waring, Bioorg. Med. Chem. Lett. 17 (2007) 82–85.
[23] G.R. Pettit, J.C. Collins, J.C. Knight, B.C. Herald, R.A. Nieman, M.D. Williams, R.K. Pettit, J. Nat. Prod. 66 (2003) 544–547.
[24] (a) A.P. Krapcho, M.E. Petry, Z. Getahun, J.J. Landi Jr., J. Stallman, J.F. Polsenberg, C.E. Gallagher, M.J. Maresch, M.P. Hacker, J. Med. Chem. 37 (1994) 828–837;
(b) J.A. Valderrana, M.F. González, D. Pessoa-Mahana, R.A. Tapia, H. Fillion, F. Pautet, J.A. Rodriguez, C. Theoduloz, G. Schmeda-Hirschmann, Bioorg. Med. Chem. 14 (2006) 5003–5011.
[25] B.A. Czeskis, J. Label Compd. Radiopharm. 39 (1997) 49–58.
[26] H. Young Choi, D. Yoon Chi, Tetr. Lett. 60 (2004) 4945–4951.
[27] J. Kim, S. Felts, L. Llauger, H. He, H. Huezo, N. Rosen, G. Chiosis, J. Biomol. Screen. 9 (2004) 375–381.
[28] D.B. Solit, G. Chiosis, Drug Discov. Today 13 (2008) 38–43.
[29] (a) L.R. Kelland, S.Y. Sharp, P.M. Rogers, T.G. Myers, P. Workman, J. Natl. Cancer Inst. 91 (1999) 1940–1949;
(b) W. Guo, P. Reigan, D. Siegel, J. Zirrolli, D. Gustafson, D. Ross, Cancer Res. 65 (2005) 10006–10015;
(c) W. Guo, P. Reigan, D. Siegel, J. Zirrolli, D. Gustafson, D. Ross, Mol. Pharmacol. 70 (2006) 1194–1203.
[30] A.M. Lewis, M. Ough, M.M. Hinkhouse, M.S. Tsao, L.W. Oberley, J.J. Cullen, Mol. Carcinog 43 (2006) 215–224 (and refs. quoted therein).
[31 W. Guo, D. Siegel, D. Ross, J. Pharm. Sci. 97 (2008) 5147–5157.
[32] A.C. Maroney, J.J. Marugan, T.M. Mezzasalma, A.N. Barnakov, T.A. Garrabrant, L.E. Weaner, W.J. Jones, L.A. Barnakova, H.K. Koblish, M.J. Todd, Biochemistry 45 (2006) 5678–5685.
[33] D. Siegel, B. Shieh, C. Yan, J.K. Kepa, D. Ross, J. Pharm. Exp. Ther. 336 (2011) 874–880.
[34] For a recent review see R. Beck, N. Dejeans, C. Glorieux, R.C. Pedrosa, D. Vásquez, J.A. Valderrama, P.B. Calderon, J. Verrax, Curr. Med. Chem. 18 (2011) 2816–2825.
[35] T. Taldone, D. Zatorska, P.D. Patel, H. Zong, A. Rodina, J.H. Ahn, K. Moulick, M.L. Guzman, G. Chiosis, Bioorg. Med. Chem. 19 (2011) 2603–2614.
[36] S.L. Dixon, A.M. Smondyrev, E.H. Knoll, S.N. Rao, D.E. Shaw, R.A. Friesner, J. Comput.-Aided Mol. Des 20 (2006) 647–671.
[37] Phase, Version 3.2. User Manual, Schrodinger, LLC, New York, 2005.
[38] Maestro, Version 9.1, Schrodinger, LLC, New York, 2005.
[39] MacroModel, Version 9.8, Schrodinger, LLC, New York, 2005.
[40] Phase, Version 3.2, Schrödinger, LLC, New York, 2005.
[41] V. Zuco, C. Zanchi, G. Cassinelli, C. Lanzi, R. Supino, C. Pisano, R. Zanier, V. Giordano, E. Garattini, F. Zunino, Cell Death Differ. 11 (2004) 280–289.